β Cell tone is defined by proglucagon peptides through cAMP signaling

Megan E. Capozzi,[1] Berit Svendsen,[1] Sara E. Encisco,[1] Sophie L. Lewandowski,[2] Mackenzie D. Martin,[1] Haopeng Lin,[3] Justin L. Jaffe,[1] Reilly W. Coch,[1,4] Jonathan M. Haldeman,[1,5] Patrick E. MacDonald,[3] Matthew J. Merrins,[2] David A. D'Alessio,[1,4] and Jonathan E. Campbell[1,4,5]

[1]Duke Molecular Physiology Institute, Duke University, Durham, North Carolina, USA. [2]Department of Medicine, Division of Endocrinology, Diabetes & Metabolism, University of Wisconsin–Madison, Madison, Wisconsin, USA. [3]Department of Pharmacology and Alberta Diabetes Institute, University of Alberta, Alberta, Canada. [4]Department of Medicine and [5]Department of Pharmacology and Cancer Biology, Duke University, Durham, North Carolina, USA.

Paracrine interactions between pancreatic islet cells have been proposed as a mechanism to regulate hormone secretion and glucose homeostasis. Here, we demonstrate the importance of proglucagon-derived peptides (PGDPs) for α to β cell communication and control of insulin secretion. Signaling through this system occurs through both the glucagon-like peptide receptor (Glp1r) and glucagon receptor (Gcgr). Loss of PGDPs, or blockade of their receptors, decreases insulin secretion in response to both metabolic and nonmetabolic stimulation of mouse and human islets. This effect is due to reduced β cell cAMP and affects the quantity but not dynamics of insulin release, indicating that PGDPs dictate the magnitude of insulin output in an isolated islet. In healthy mice, additional factors that stimulate cAMP can compensate for loss of PGDP signaling; however, input from α cells is essential to maintain glucose tolerance during the metabolic stress induced by high-fat feeding. These findings demonstrate an essential role for α cell regulation of β cells, raising the possibility that abnormal paracrine signaling contributes to impaired insulin secretion in diabetes. Moreover, these findings support reconsideration of the role for α cells in postprandial glucose control.

Introduction

Dysfunction of the pancreatic islet is central to the pathogenesis of diabetes, and insufficient insulin release from islet β cells is the essential component for disease development (1). There is also evidence to support excess glucagon release from islet α cells in persons with type 2 diabetes (T2D) as a factor that contributes to hyperglycemia (2). Physiologic regulation of islet hormone secretion is generally attributed to plasma nutrients, particularly glucose and aa, as well as circulating insulinotropic hormones, termed incretins (3, 4). However, over the last several decades, communication among islet cell types has emerged as critical in the control of pancreatic endocrine function. For example, β cells secrete several products that inhibit glucagon release from α cells (5), and islet δ cells serve a multifaceted role in paracrine inhibition of α and β cell secretion (6, 7). However, a key interaction that has not been explored in great depth is α to β cell communication, although several older, and recent, studies support the importance of this axis for β cell function (8–13). β cells express the glucagon receptor (Gcgr), a family-B GPCR that has significant homology and functional overlap with the receptors for the incretins, glucose-dependent insulinotropic polypeptide (GIP) and glucagon-like peptide 1 (GLP-1) (14). Moreover, it is well established that pharmacologic administration of glucagon stimulates insulin secretion (15–17), and recent work supports glucagon as a key species-specific determinant of glycemic set point (12). Despite this body of experimental data, the importance of paracrine stimulation of β cell secretion by α cells remains unclear, and the mechanism by which α cells communicate with cells has not been conclusively established. Several recent papers suggest that α cell production of GLP-1 mediates this signal (18, 19); yet previous observations that glucagon stimulates insulin secretion through both the β cell Gcgr and GLP-1 receptor (Glp1r) (13, 15) add a further layer of complexity to the process. Finally, it is unknown what physiological conditions would evoke α to β cell communication to stimulate insulin secretion. These gaps in knowledge, and the prominent role of circulating glucagon to promote hepatic glycogenolysis and gluconeogenesis and raise blood glucose (20), have

obscured paracrine actions of proglucagon-derived peptides (PGDPs) on β cells. Here, we demonstrate that (a) α to β cell communication is necessary for a normal quantitative insulin response to both nutrient and nonnutrient β cell depolarization; (b) PGDPs control the tone of insulin secretion by establishing β cell levels of cAMP; (d) a subset of aa utilize PGDPs from α cells to stimulate insulin secretion; and (e) PGDP input is necessary for the β cell adaptations that maintain glucose tolerance in response to high-fat feeding.

Results

We sought to test the importance of α to β cell communication by generating a mouse line with a β cell–specific deletion of the Gcgr (*Gcgr*$^{βcell–/–}$ mice; Supplemental Figure 1A; supplemental material available online with this article; https://doi.org/10.1172/jci.insight.126742DS1) (21). Islets isolated from littermate controls and *Gcgr*$^{βcell–/–}$ mice perifused with graded doses of glucagon displayed identical insulin secretion profiles (Figure 1A), suggesting that the Gcgr is dispensable for glucagon-stimulated insulin secretion. Consistent with these findings, *Gcgr*$^{βcell–/–}$ mice had glycemic excursions and glucose clearance comparable to that of WT controls in response to oral and i.p. glucose challenges (Supplemental Figure 1, B and C). Moreover, a highly specific Gcgr agonist failed to stimulate insulin secretion in *Gcgr*$^{βcell–/–}$ islets (Supplemental Figure 2A), confirming a functional Gcgr knockout. Since glucagon-stimulated insulin secretion can be blocked with an antagonist of the Glp1r (15), we pursued this alternative pathway for glucagon signaling. The Glp1r antagonist exendin 9–39 (Ex9) reduced glucagon-stimulated insulin secretion by approximately 65% in WT islets and approximately 80% in *Gcgr*$^{βcell–/–}$ islets (Figure 1A), indicating that the Glp1r is the principal mediator of glucagon-stimulated insulin secretion. To validate this conclusion, we performed the reciprocal experiment using a Gcgr antagonist (GRA) and *Glp1r*$^{βcell–/–}$ islets (22). In this experiment, β cell deletion of the Glp1r reduced glucagon-stimulated insulin secretion by approximately 75%, whereas the GRA in WT islets did not have an effect (Figure 1B). However, the addition of GRA exposure in *Glp1r*$^{βcell–/–}$ islets attenuated glucagon-stimulated insulin secretion to about 85% of normal. Together, these results corroborate previous reports that glucagon can stimulate insulin secretion through both the Gcgr and the Glp1r (13, 15) but show that glucagon signaling through the β cell Glp1r is more important.

Although we tested a broad range of glucagon concentrations to measure glucagon-stimulated insulin secretion, it is not clear which of these are reflective of the concentrations within the islet, where paracrine α to β cell communication would take place. To gain insight into the paracrine effects of glucagon, we perifused islets with the aa arginine and glutamine, which are known to stimulate glucagon secretion (23–25). Both aa stimulated α cells to secrete glucagon (Figure 1C) and GLP-1 (Figure 1C, insets) but failed to stimulate insulin secretion from β cells at low-glucose conditions (Supplemental Figure 2, B and C), indicating that these concentrations of aa do not have a direct, glucose-independent effect on β cells. While less GLP-1 was released from perifused α cells than glucagon (Figure 1C), it was approximately 300 times more potent as an insulin secretagogue (Supplemental Figure 2, D and E). Therefore, it is possible that both peptides act as local insulinotropins in the islet, as previously reported (18, 19). To test the contribution of endogenously produced PGDPs for β cell function, we perifused islets with aa at high-glucose conditions and interrupted α to β cell communication using complementary strategies. Insulin secretion stimulated by aa was intact in islets from *Gcgr*$^{βcell–/–}$ and *Glp1r*$^{βcell–/–}$ mice (Supplemental Figure 3, A and B), whereas pharmacological antagonism of either the Gcgr or Glp1r reduced aa-stimulated insulin secretion (Supplemental Figure 3, C and D). Remarkably, simultaneously blockade of both Gcgr and Glp1r using genetic knockouts and pharmacological antagonists nearly abolished aa-stimulated insulin secretion (Figure 1, D and E). These findings indicate that PGDPs are essential for aa-stimulated insulin secretion, that both the Gcgr and Glp1r can mediate this effect, and that compensation occurs for single receptor gene deletions that is not seen with acute pharmacologic blockade.

To further investigate α cell regulation of β cell function, we measured insulin secretion by islets from a line of mice with genetic disruption of *Gcg* expression; these animals lack production of all PGDPs, including glucagon and GLP-1 (*Gcg*$^{–/–}$ mice) (26). Consistent with findings using interruption of Gcgr and Glp1r signaling, loss of the ligands for these receptors also severely blunted aa-stimulated insulin secretion (Figure 2A and Supplemental Figure 3E). Remarkably, islets from *Gcg*$^{–/–}$ mice also had dramatically reduced glucose-stimulated insulin secretion (GSIS) (Figure 2A). One explanation for this effect may be the loss of the acute rise in glucagon and GLP-1 release observed in WT islets after transitioning from low- to high-glucose conditions (3–8 minutes in Figure 1C), before the marked suppression of α cell output typically seen with hyperglycemia (8–30 minutes in Figure 1C).

To determine whether germ-line deletion of *Gcg* leads to a general impairment of β cell function, we stimulated insulin secretion with insulinotropic GPCR ligands: glucagon, GLP-1, and GIP. All three peptides stimulated insulin secretion comparably in WT and *Gcg*$^{-/-}$ islets (Figure 2A), demonstrating that provision of ligands for these GPCRs restores insulin secretion and suggesting that the insulin secretory defect in the *Gcg*$^{-/-}$ islets is specific to loss of PGDPs. To confirm this, we used adenovirus-mediated delivery of Cre recombinase ex vivo to cleave the floxed stop codon in the *proglucagon* promoter of *Gcg*$^{-/-}$ islets and allow normal *Gcg* transcription (26). The Cre-mediated restoration of *Gcg* transcription within the islet restored α cell synthesis of glucagon and GLP-1 to WT levels (Supplemental Figure 3F) and completely rescued glucose- and aa-stimulated insulin secretion (Figure 2B); control virus–treated (β-gal–treated) *Gcg*$^{-/-}$ islets continued to display impaired nutrient-stimulated insulin secretion compared with WT islets (Supplemental Figure 3G). To confirm that the marked reduction of glucose- and aa-stimulated insulin secretion is the result of impaired α to β cell communication, rather than dysfunctional β cells per se, WT islets were treated with Ex9 and GRA to block both the Glp1r and Gcgr acutely. Dual receptor blockade led to significant attenuation of glucagon-stimulated insulin secretion (Figure 2C), aa-stimulated insulin (Figure 2D), and GSIS (Figure 2, C and D) but not GIP-stimulated insulin secretion (Figure 2C). The normal response to GIP in islets treated with Ex9/GRA highlights that sufficient cAMP signaling can overcome the reduction in nutrient-stimulated insulin secretion brought about by antagonizing the receptors for PGDPs. Together, these findings demonstrate that PGDPs are necessary for nutrient-stimulated insulin secretion in isolated islets.

The current working model of GSIS divides the stimulatory effect of glucose into *triggering* (the effect of glucose to cause β cell membrane depolarization and increase intracellular calcium) and *amplifying* (the effect of glucose to augment insulin release at a given calcium concentration) phases (27). To determine if proglucagon-mediated β cell signaling differentially affects triggering versus amplification pathways (27), WT and *Gcg*$^{-/-}$ islets were perifused with diazoxide (Dz) and KCl at low-glucose conditions to assess triggering or at high-glucose conditions to assess metabolic amplification (Figure 3). The insulin profiles from *Gcg*$^{-/-}$ islets had similar dynamics to controls but markedly reduced insulin responses under both low- and high-glucose conditions. While both the triggering and amplifying components of insulin secretion were present, suggesting that the fundamental processes governing these events remained intact, the amount of insulin secreted was severely attenuated in the absence of PGDPs. This result suggests that signaling through the Gcgr and/or Glp1r controls the gain in β cells, establishing an intracellular tone that governs quantitative insulin release.

The cardinal mechanism by which stimulatory family-B GPCRs, such as the Gcgr and Glp1r, signal is through G_s activation of adenylyl cyclase and production of cAMP. This led us to hypothesize that the reduced insulin secretion following impaired α to β cell communication is due to inadequate cAMP production. Indeed, cAMP antagonism with Rp-8-Br-cAMPS-pAB has been reported to decrease GSIS in human islets (28), and defective cAMP signaling contributes to impaired insulin secretion in *Glp1r*$^{-/-}$ islets (29) or in response to lipotoxicity (30). Consistent with our hypothesis, cAMP levels were decreased dramatically in β cells acutely treated with Ex9/GRA, as determined by using a cAMP biosensor (Figure 4A). We also found that Ex9/GRA treatment reduced Ca^{2+} levels during low-glucose, high-glucose, and KCl conditions (Figure 4B), along with a subtle reduction in the Ca^{2+} responses to high glucose or KCl (determined by the reduction in incremental AUCs for each condition). However, the Ca^{2+} responses in islets treated with Ex9/GRA retained a similar pattern in the response to glucose or KCl compared with control conditions. A comparison of WT and *Gcg*$^{-/-}$ islets reveal a similar decrease in the Ca^{2+} response to glucose but not KCl in the knockout line (Figure 4C). The Ca^{2+} responses in both models are compatible with the results of the Dz/KCl experiment (Figure 3), where lack of proglucagon input did not change the dynamics of insulin secretion regulated by changes in Ca^{2+} but instead decreased the quantity of insulin secretion under all conditions, consistent with diminished β cell tone. Moreover, the impaired insulin secretion in response to 30 mM KCl (Figure 3), despite sustained Ca^{2+} in *Gcg*$^{-/-}$ islets (Figure 4C), illustrates that cAMP affects other signaling pathways in addition to the regulation of Ca^{2+} levels. This also indicates that pathways independent of proglucagon signaling exert a significant influence on Ca^{2+} levels. To further validate the role of cAMP, we treated WT and *Gcg*$^{-/-}$ islets with the phosphodiesterase inhibitor isobutylmethylxanthine (IBMX) to prevent the degradation of intracellular cAMP. While IBMX activated PKA signaling in WT islets, both basal and stimulated PKA levels were significantly attenuated in *Gcg*$^{-/-}$ islets (Figure 4D). Perifusion of WT islets with IBMX increased insulin secretion in a dose-dependent manner but had a minimal effect on *Gcg*$^{-/-}$ islets (Figure 4E). To demonstrate that decreased insulin secretion from *Gcg*$^{-/-}$ islets is due to insufficient cAMP levels, rather than impaired cAMP signaling, we perifused islets
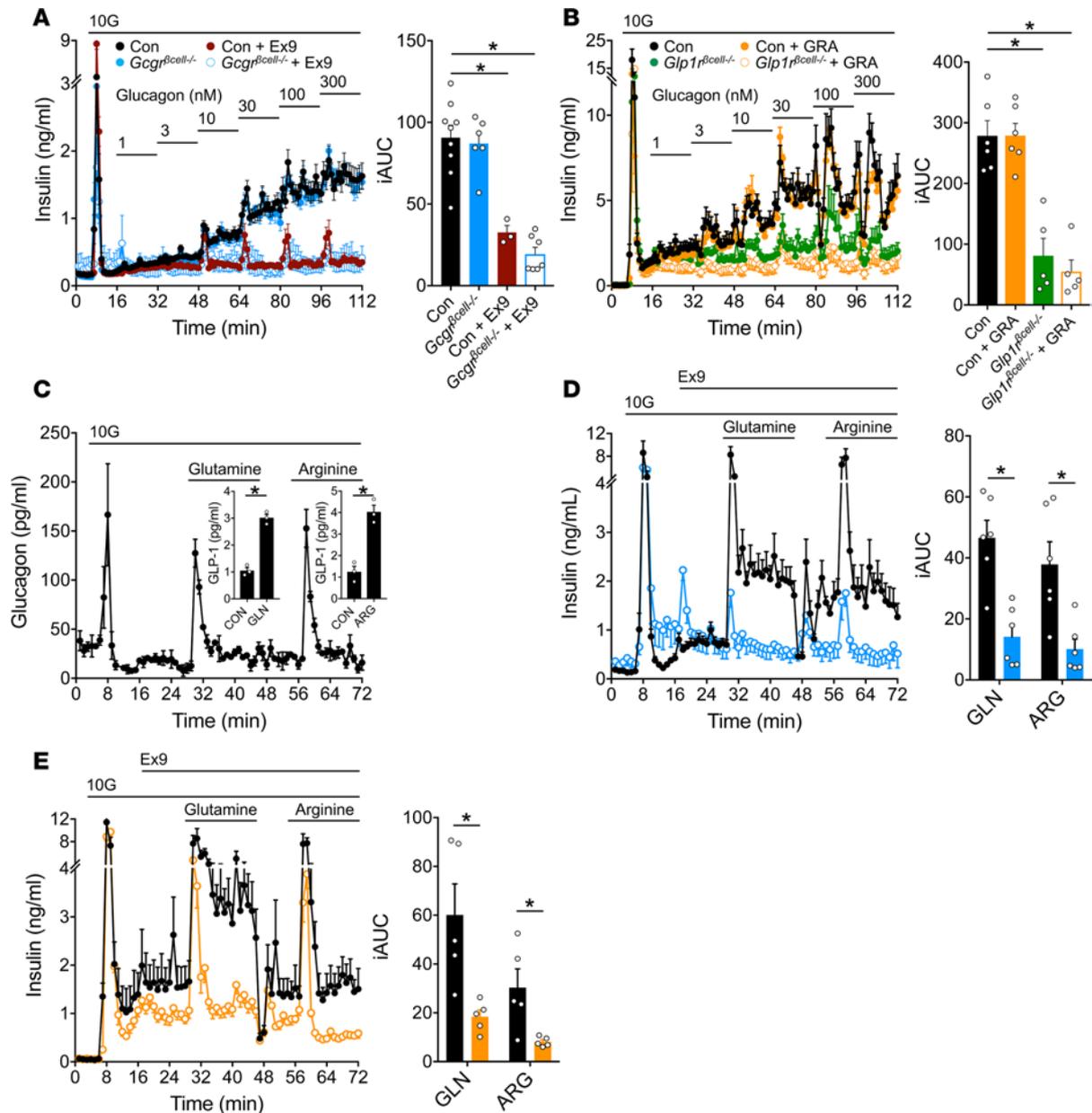
Figure 1. Proglucagon products stimulate insulin secretion through both the Glp1r and Gcgr. (**A**) Insulin secretion in response to increasing doses of glucagon in control (Con; *MIP-Cre^ERT*) or *Gcgr^βcell-/-* islets with or without 1 μM exendin 9–39 (Ex9) (Con, *Gcgr^βcell-/-*, Con + Ex9, *Gcgr^βcell-/-* + Ex9; n = 9, 8, 3, 7). (**B**) Insulin secretion in response to increasing doses of glucagon from Con or *Glp1r^βcell-/-* islets with or without 10 μg/ml GRA (Con, Con + GRA, *Glp1r^βcell-/-*, *Glp1r^βcell-/-* + GRA; n = 6, 6, 5, 5). (**C**) Glucagon and total GLP-1 secretion in response to 10 mM glutamine and 1 mM arginine (n = 3). (**D**) Insulin secretion in response to 10 mM glutamine and 1 mM arginine from Con or *Gcgr^βcell-/-* islets treated with 1 μM Ex9 (n = 6). (**E**) Insulin secretion in response to 10 mM glutamine and 1 mM arginine from WT or *Glp1r^βcell-/-* islets treated with 10 μg/ml GRA (n = 5). *P < 0.05. Data are shown as mean ± SEM. Data were analyzed with a 2-way ANOVA for the iAUCs (**A**, **B**, **D**, and **E**) or a 2-tailed Student's *t* test (**C**).

with increasing concentrations of the adenylyl cyclase activator forskolin (FSK). In this paradigm, both WT and *Gcg^-/-* islets had identical insulinotropic responses to increasing concentrations of FSK (Figure 4F). Taken together with the findings from experiments using GIP to stimulate insulin during the blockade of Gcgr and Glp1r (Figure 2C), this result suggests that alternative means of stimulating cAMP can compensate for the interruption of α to β cell signaling. To confirm this inference, we assessed exocytosis in individual patch-clamped β cells from WT and *Gcg^-/-* islets in the presence or absence of cAMP. Notably, in the absence of cAMP, both WT and *Gcg^-/-* β cells had similar markedly reduced exocytosis (Figure 4G). However, the addition of cAMP to the patch pipette increased exocytosis to comparable levels in both sets of β cells (Figure 4G). These results establish a mechanism whereby deficient cAMP signaling
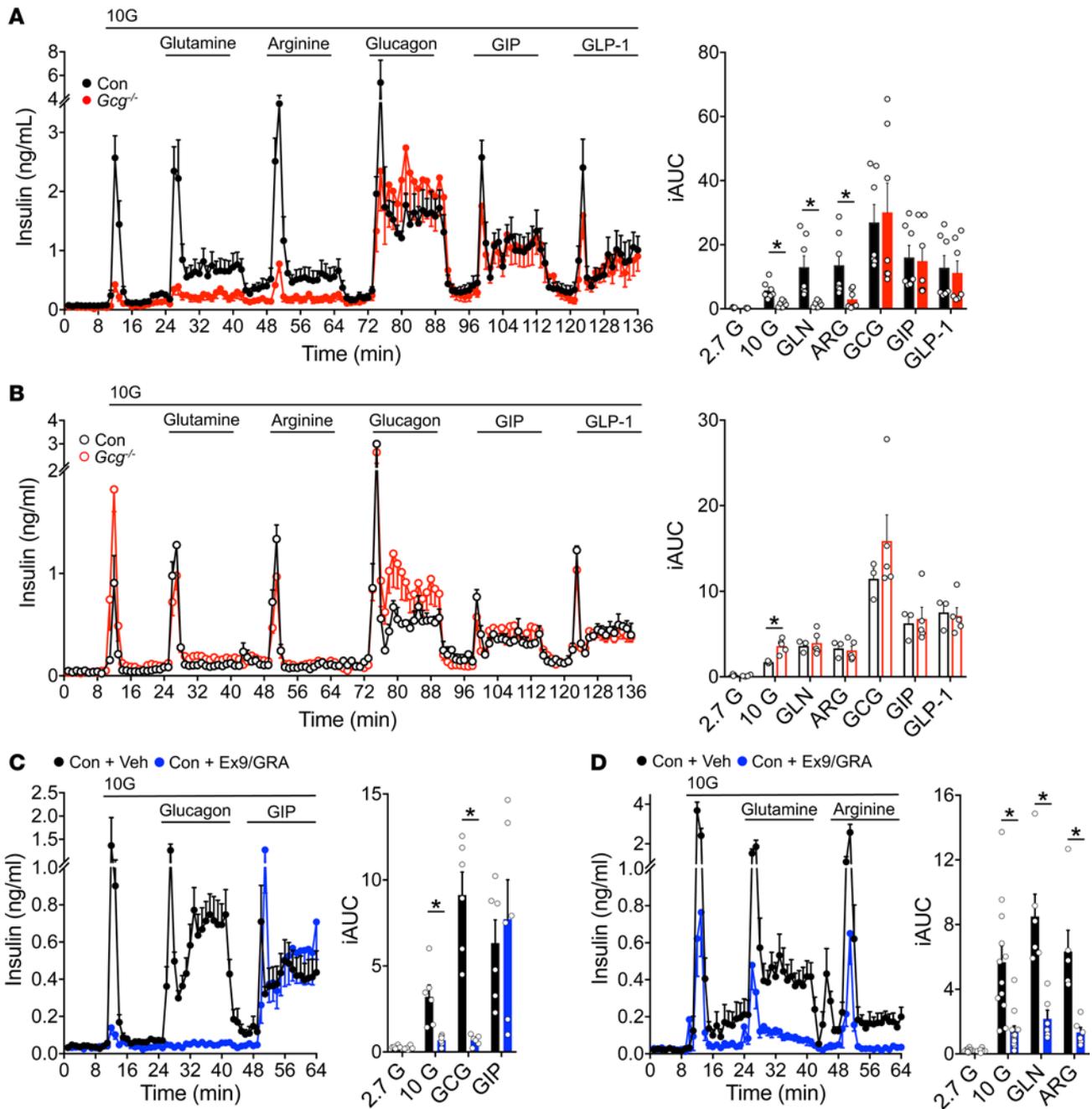
Figure 2. Proglucagon products are necessary for nutrient-stimulated insulin secretion. (A) Insulin secretion in response 10 mM glucose, 10 mM glutamine, 1 mM arginine, 10 nM glucagon, 3 nM GIP, and 0.3 nM GLP-1 from WT or Gcg^{null} islets ($n = 7$). **(B)** Insulin secretion in response 10 mM glucose, 10 mM glutamine, 1 mM arginine, 10 nM glucagon, 3 nM GIP, and 0.3 nM GLP-1 from WT + Ad-CMV-Cre ($n = 3$) or Gcg^{null} + Ad-CMV-Cre islets ($n = 5$). **(C)** Insulin secretion in response to 10 mM glucose, 10 nM glucagon, and 3 nM GIP from WT islets with or without 1 μM Ex9 and 10 μg/ml GRA ($n = 6$). **(D)** Insulin secretion in response to 10 mM glucose, 10 mM glutamine, and 1 mM arginine from WT islets with or without 1 μM Ex9 and 10 μg/ml GRA ($n = 6$). *$P < 0.05$. Data are shown as mean ± SEM. Data were analyzed by a 2-way ANOVA of the iAUCs.

accounts for the severe defect in nutrient-stimulated insulin secretion observed in the absence of PGDPs. In total, these experiments indicate that the attenuation of insulin secretion arising from impaired α to β cell communication can be ameliorated by mechanisms that augment cAMP production.

Human islet architecture has notable differences from that of rodent islets in ways that support greater α/β cell paracrine signaling (31). First, α cells constitute a higher percentage of human islet cells, almost equal to cells, while the α/β cell ratio in mice is closer to 1 to 4. Second, α cells are interspersed throughout the human islet (31), with a large percentage of α cells juxtaposed to a neighboring β cell; in mice, α cells are situated on the

JCI insight
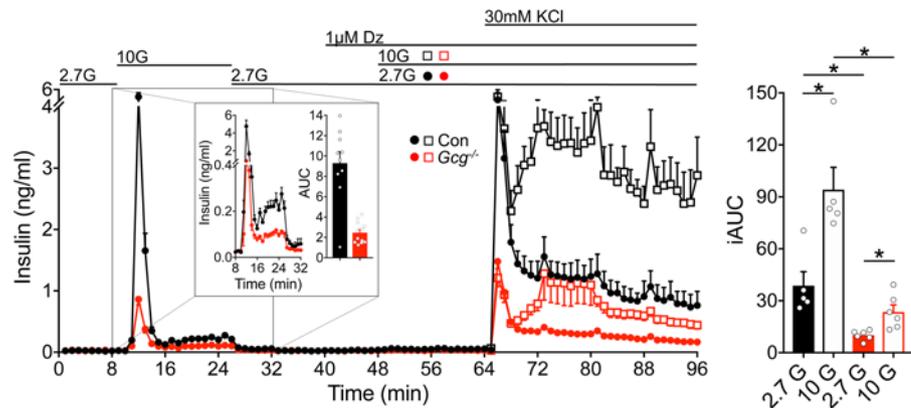
Figure 3. Lack of proglucagon peptide input reduces insulin secretion in response to both triggering and amplification signals. Insulin secretion in response to different concentrations of 2.7 mM glucose, 10 mM glucose, 400 μM diazoxide (Dz), or Dz with 30 mM KCl, as indicated from WT (*n* = 5) or *Gcg^null^* islets (*n* = 6). Data are shown as mean ± SEM. Data were analyzed by a 2-way ANOVA of the iAUCs or a 2-tailed Student's *t* test (inset).

periphery of the islet with less contact to β cells. It is notable that human islets have higher insulin stimulated responses, particularly nutrients, compared with rodent islets (3), and human islets transplanted into mice establish a lower ambient glycemia than rodent islets (12). We tested the importance of α to β cell communication in human islets using the pharmacological antagonists that were effective in mice and found that Ex9/GRA significantly inhibited aa- and GSIS (Figure 5A); these treatments also caused an acute rise in glucagon release (Supplemental Figure 4A). Notably, the combination of inhibitors is required to block glucagon-stimulated insulin secretion in human islets, as individual receptor blockade had limited effect (Supplemental Figure 4, B and C). Similar to murine islets, Ex9/GRA blunted both the triggering and metabolic amplification components of insulin release (Figure 5B). Also consistent with the results from mouse islets, IBMX could not potentiate insulin secretion normally in the presence of Ex9/GRA (Figure 5C), suggesting a defect in cAMP generation similar to that observed in mice. While GRA/Ex9 completely blocked glucagon-stimulated insulin secretion, the insulin response to GIP remained intact (Figure 5D), substantiating our mouse experiments, which show that alternative activation of G_s/adenylyl cyclase/cAMP maintains insulin secretion.

Remarkably, Ex9/GRA treatment lowered insulin secretion in the early phases of our perifusions performed at basal glucose levels (2.7 mM) in the majority of human donors (Figure 5, A and C). To investigate this further, we added Ex9/GRA during extended perifusion of 2.7 mM glucose and observed a dramatic decrease of insulin secretion (Figure 5E); insulin secretion remained lower as glucose concentrations were raised (Figure 5F). Moreover, glucagon, incretins, and aa all stimulated insulin secretion at low-glucose concentration in human islets (Supplemental Figure 4, F and G), a finding not seen in mouse islets (Supplemental Figure 2, B and C). Thus, in humans, α cells have the potential to regulate β cell tone across a wider range of glucose concentrations, including those mimicking fasting. In humans, fasting insulin secretion is proportional to systemic insulin sensitivity (32), an association that has not been explained. Our findings raise the possibility that α cells link insulin needs with insulin provision.

To determine the effect of β cell PGDP receptors in vivo, a setting where additional G_s GPCR ligands from outside the islet can contribute to the levels of cAMP, we generated mice with conditional deletion of *Gcgr* and *Glp1r* from the β cell (*Gcgr;Glp1r^βcell−/−^* mice). Lean chow-fed *Gcgr;Glp1r^βcell−/−^* mice had similar glucose tolerance to control mice in response to both i.p. and oral glucose loads (Figure 6, A and B), indicating that the β cell receptors for PGDPs are dispensable in young, healthy mice. However, when *Gcgr;Glp1r^βcell−/−^* mice were chronically exposed to a high-fat diet and developed obesity, a different profile emerged. Metabolically stressed *Gcgr;Glp1r^βcell−/−^* mice were profoundly glucose intolerant in response to i.p. glucose compared with controls (Figure 6C). Moreover, fasting glycemia and the glucose excursion following an oral glucose challenge were also significantly higher in obese *Gcgr;Glp1r^βcell−/−^* mice compared with controls (Figure 6D), which had comparable body weights and levels of insulin sensitivity (Supplemental Figure 5). The somewhat muted difference during an oral glucose tolerance test compared with i.p. glucose led us to reason that a gut-derived GPCR ligand, such as GIP, could compensate for lack of PGDP signaling to preserve β cell function.
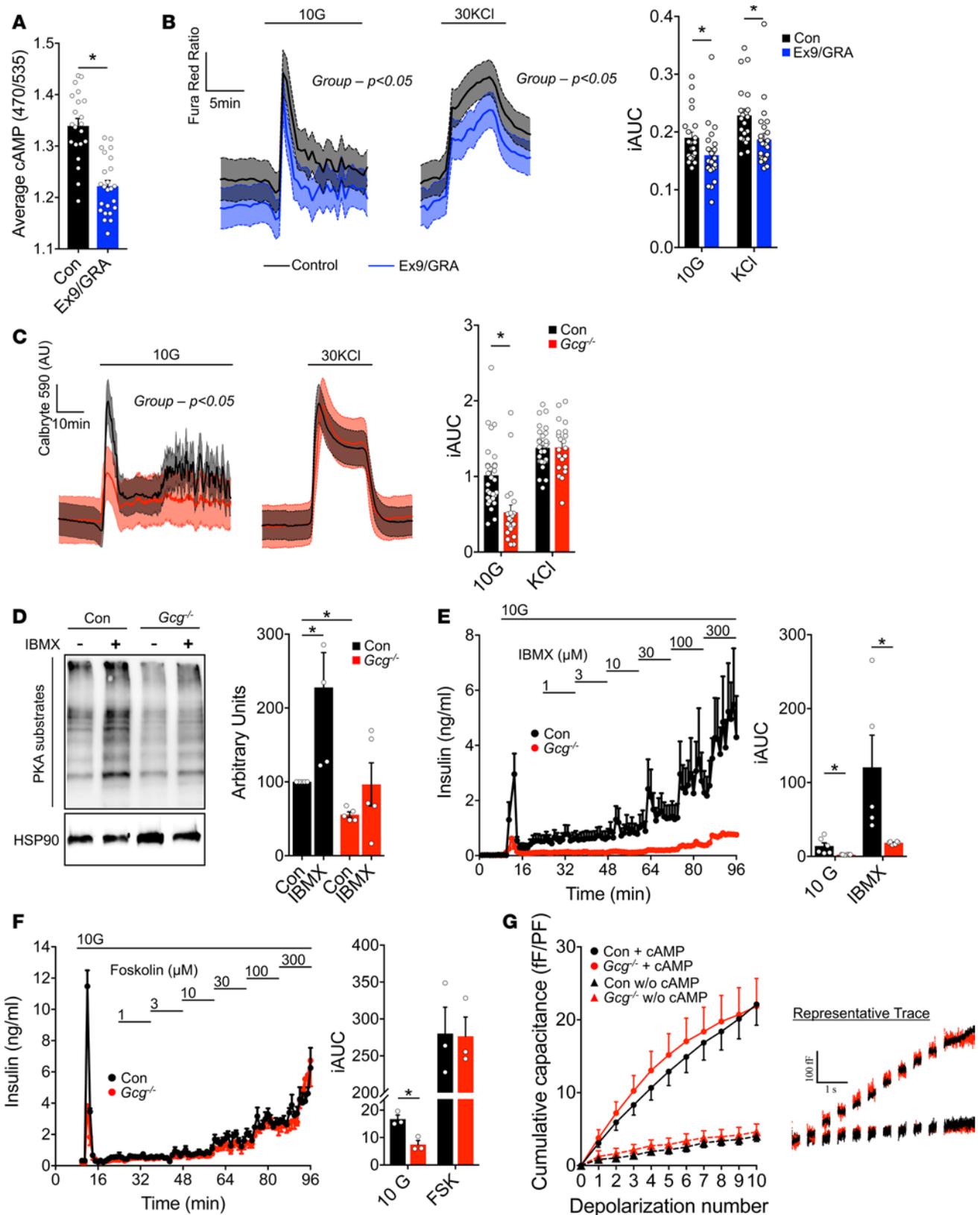
Figure 4. Impaired proglucagon input reduces cAMP signaling in β cells. (**A**) Average cAMP levels from WT islets acutely exposed to either control (*n* = 21) or Ex9/GRA (*n* = 24) conditions. (**B**) Cytosolic Ca²⁺ levels in WT islets acutely exposed to either control (*n* = 21) or Ex9/GRA (*n* = 24) conditions in response to 10 mM glucose or 30 mM KCl. (**C**) Cytosolic Ca²⁺ levels in WT (*n* = 30) and *Gcg⁻/⁻* (*n* = 21) islets in response to 10 mM glucose or 30 mM KCl. (**D**) Phosphorylation of PKA substrates and HSP90 protein levels from WT (*n* = 7) or *Gcg⁻/⁻* islets (*n* = 7). (**E**) Insulin secretion in response to increasing doses of IBMX in WT (*n* = 6) or *Gcg⁻/⁻* islets (*n* = 6) at 10 mM glucose. (**F**) Insulin secretion in response to increasing doses of FSK in WT or *Gcg⁻/⁻* islets (*n* = 3) at 10 mM glucose. (**G**) Cumulative capacitance from sequential depolarization in individual β cells from WT or *Gcg⁻/⁻* islets with

or without cAMP (left) and representative trace of depolarizations (right). (Con + cAMP, $Gcg^{-/-}$ + cAMP, Con, $Gcg^{-/-}$; n = 38, 38, 34, 37) *$P < 0.05$. Data are shown as mean ± SEM. Data were analyzed by a 2-way ANOVA of the iAUCs.

We hypothesized that GIP sensitivity is enhanced in the islets of $Gcgr;Glp1r^{\beta cell-/-}$ mice and compensates for the lack of PGDP input because $Glp1r$ deletion has previously been shown to confer increased GIP sensitivity (33). To that end, we observed that $Gcgr;Glp1r^{\beta cell-/-}$ mice had a greater decrease of glycemia than controls when given exogenous GIP (Figure 7, A and B) and that perifused islets from $Gcgr:Glp1r^{\beta cell-/-}$ mice secreted more insulin in response to GIP (Figure 7C). Notably, perifused islets from $Gcgr:Glp1r^{\beta cell-/-}$ mice phenocopied the impaired GSIS and aa-stimulated insulin secretion observed from $Gcg^{-/-}$ islets or islets treated with pharmacologic inhibitors. The compensatory increase in GIP sensitivity in $Gcgr;Glp1r^{\beta cell-/-}$ mice may be the factor preserving normal glucose tolerance in young, healthy mice. In this context, it is important to consider that chronic hyperglycemia in T2D renders humans unresponsive to GIP, even at pharmacological levels (34), while also decreasing the expression of *GLP1R* and the insulin response to physiological levels of GLP-1 (35, 36), suggesting impaired β cell signaling.

Discussion

The actions of GPCR ligands in the control of insulin secretion have been known for decades. The hallmark example of this is the incretin effect, attributed to GIP and GLP-1 and accounting for up to 70% of postprandial insulin secretion (37). Furthermore, it is commonly accepted that the incretin effect is significantly diminished in T2D (36), linking decreased GPCR signaling with insufficient insulin secretion and hyperglycemia. Over the past 2 decades new therapeutic agents that target incretin receptors on β cells have been one of the major advances in diabetes care, providing clinical evidence that activation of GPCRs on β cells can improve insulin secretion and reduce glycemia. However, recent findings, including those presented here, challenge the conventional model of incretin action. This model holds that GPCR regulation of insulin secretion begins with nutrient-stimulated release of GIP and GLP-1 from enteroendocrine cells in the intestine and emphasizes hormonal action of these gut-derived ligands on prandial insulin release (4). Recent evidence from preclinical models indicates that Glp1r activation is critical even in the absence of nutrient-stimulated GLP-1 (22) and that pancreatic rather than intestinal proglucagon reexpression $Gcg^{-/-}$ has the more important effect on glycemic regulation (26). These findings are consistent with local, paracrine actions of PGDPs, which include glucagon (Figure 1, A and B) (13, 15) as well as GLP-1 (Figure 1C) and potentially other PGDPs, such as oxyntomodulin (38, 39). The findings presented herein define an expanded role for β cell GPCR and identify PGDP as fundamental to regulated insulin secretion.

The major findings of this paper are that PGDPs are necessary for establishing the level of cAMP in β cells, which determines the normal quantitative insulin response to both metabolic and nonmetabolic stimuli. These results add to and extend the previous findings that demonstrate the importance of α to β cell communication (8, 40–42). These were the first reports that separating β cells from the paracrine input of α cells decreases insulin secretion and lowers cAMP levels. Subsequent reports measuring insulin secretion from single and paired cells by reverse hemolytic plaque assays showed that α-β paired cells produced significantly more insulin in response to glucose that single β cells alone (9). Finally, recent evidence has supported these ideas using isolated islets (39) or a perfused pancreas (13) in mouse models.

The results reported here have several important implications that extend this area of research. First, the insulinotropic action of some aa is indirect, and their stimulation of β cells is mediated primarily through α cell ligands for the Gcgr and Glp1r. This result suggests a distinct role for α cells as islet aa sensors and is consistent with recent observations of aa effects on α cell growth and function (24, 25). In this model, the α cell is in a central position to dictate the glucagon/insulin ratio in the portal circulation before and after meals, with significant implications for glucose homeostasis. Under fasting conditions, endogenously derived aa arriving at the islet would result in a high glucagon/insulin ratio due to the reduced insulinotropic action of PGDPs at low glycemia. This ratio would facilitate gluconeogenesis and endogenous glucose production. However, under postprandial conditions, aa would stimulate both insulin and glucagon, significantly altering the glucagon/insulin ratio to favor glucose disposal.

Second, in the absence of PGDPs or Gcgr/Glp1r signaling, GSIS can be rescued by GIP or FSK. These findings emphasize the importance of G_s/adenylyl cyclase/cAMP to permit the well-established effects of glucose to fully trigger, and amplify, insulin secretion (27). Importantly, our data extend the
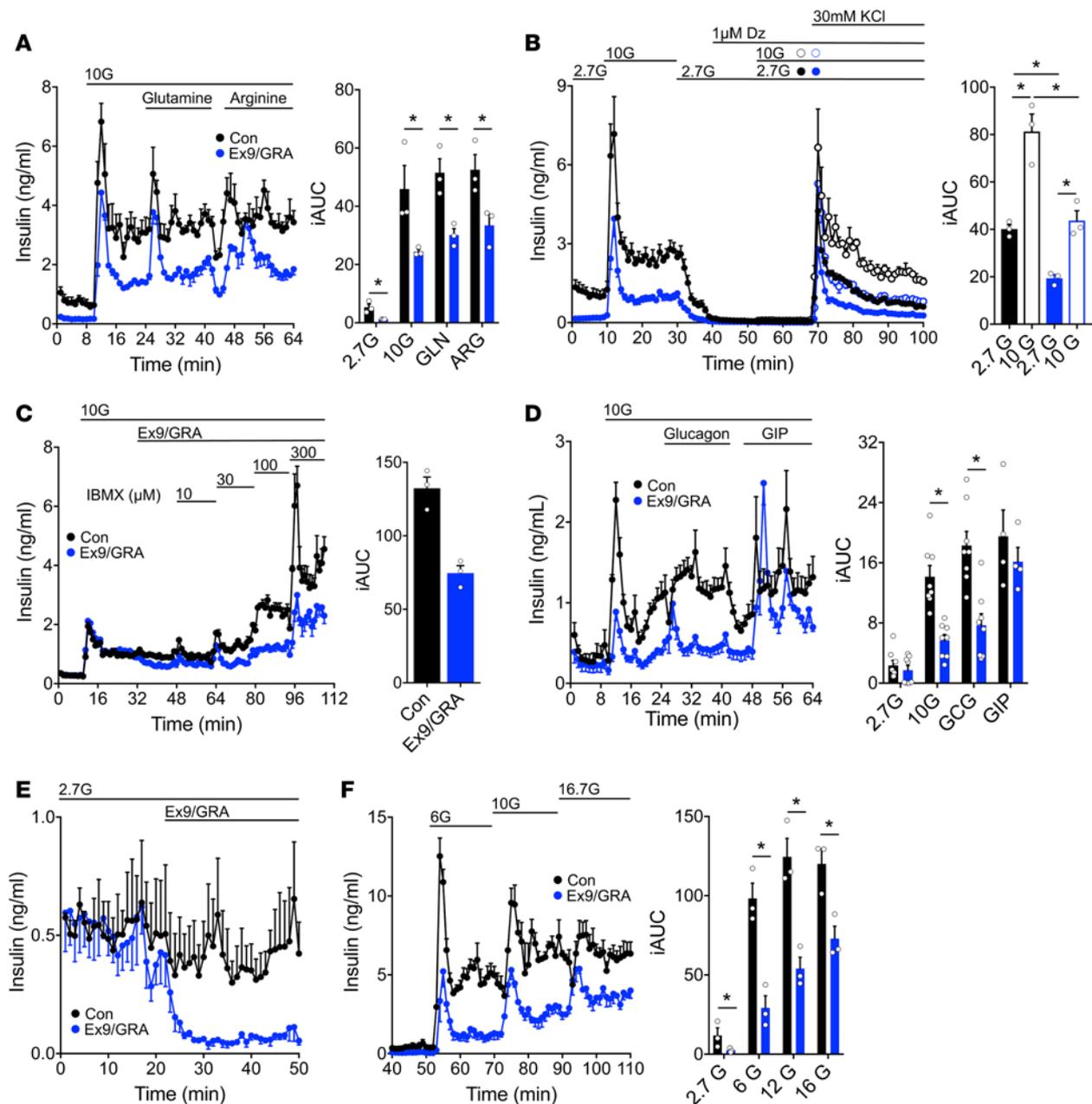
Figure 5. Proglucagon products set the tone for insulin secretion in human islets. (**A**) Insulin secretion from human islets with or without 1 μM Ex9 and 10 μg/ml GRA stimulated with 10 mM glutamine or 1 mM arginine (n = 3). (**B**) Insulin secretion in response to different combinations of 2.7 mM glucose, 10 mM glucose, 1 μM diazoxide (Dz), or Dz with 30 mM KCl, as indicated, from human islets with or without 1 μM Ex9 and 10 μg/ml GRA (n = 3). (**C**) Insulin secretion in response to increasing doses of IBMX in human islets with or without 1 μM Ex9 and 10 μg/ml GRA (n = 3). (**D**) Insulin secretion from human islets with or without 1 μM Ex9 and 10 μg/ml GRA (n = 3) stimulated with 10 nM glucagon or 50 nM GIP. (**E**) Insulin secretion from human islets with or without 1 μM Ex9 and 10 μg/ml GRA (n = 3) in response to low-glucose conditions. (**F**) Insulin secretion from human islets in response to increasing glucose concentrations with or without 1 μM Ex9 and 10 μg/ml GRA (n = 3). *P < 0.05. Data are shown as mean ± SEM. Data were analyzed by a 2-way ANOVA of the iAUCs (**A**, **B**, **D**, and **F**) or a 2-tailed Student's t test (**C**).

role of cAMP beyond potentiation of GSIS, which had been the prevailing view cAMP action in the insulin response (43). Indeed, our experiments show that the effects of cAMP are divorced from the Ca^{2+} signaling, revealing the potential for two distinct signaling pathways that govern insulin secretion. The first of these pathways is metabolism of glucose that can both trigger a β cell through depolarizing events that converge upon Ca^{2+} signaling (27) as well as dictate the level of insulin secretion through metabolic amplification (44). Our data describe a second, parallel pathway by which the level of cAMP dictates the magnitude of insulin secretion independent of the triggering and amplifying
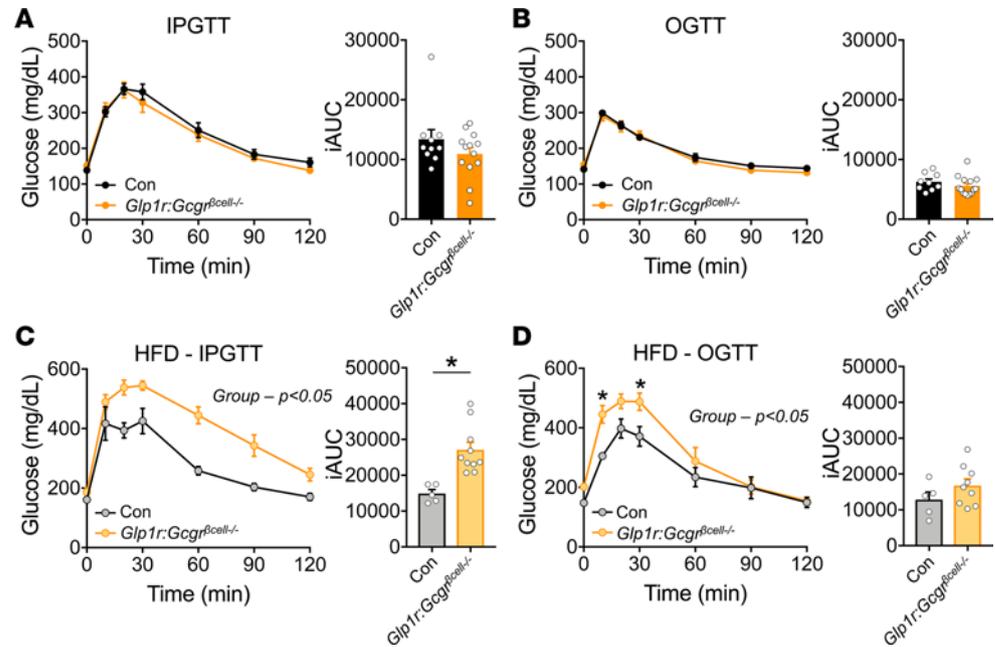
Figure 6. Loss of PGDP input into β cells combined with high-fat feeding leads to glucose intolerance. (**A**) i.p. glucose tolerance (1.5 mg/kg) and iAUC of 12- to 16-week-old chow-fed control (Con; *MIP-Cre*[ERT], *n* = 10) and *Gcgr:Glp1r*[βcell-/-] (*n* = 13) mice. (**B**) Oral glucose tolerance (1.5 mg/kg) and iAUC of 12- to 16-week-old chow-fed Con (*n* = 9) and *Gcgr:Glp1r*[βcell-/-] (*n* = 14) mice. (**C**) i.p. glucose tolerance (1.5 mg/kg) and iAUC of 20- to 24-week-old high-fat diet–fed (HFD-fed) Con (*n* = 5) and *Gcgr:Glp1r*[βcell-/-] (*n* = 10) mice. (**D**) Oral glucose tolerance (1.5 mg/kg) and iAUC of 20- to 24-week-old HFD-fed Con (*n* = 5) and *Gcgr:Glp1r*[βcell-/-] (*n* = 10) mice. *$P < 0.05$ vs. Con. Data are shown as mean ± SEM. Data were analyzed by a 2-way ANOVA of glycemic curves or a 2-tailed Student's *t* test of the iAUCs.

pathways. In isolated murine and human islets, cAMP levels are dependent on PGDP input from α cells, and this determines the amount of insulin released to a broad range of stimuli. Our data generally agree with those of previous reports that show impaired GSIS in isolated islets devoid of α cells (39) or in perfused pancreata with diminished PGDP signaling (13). Importantly, we demonstrate that the impaired β cell function extends beyond GSIS. Indeed, based on the patterns of insulin released from perifused islets, the general mechanisms of GSIS appear to be retained (Figure 3) but β cell tone is diminished and insulin profiles are diminished to a small fraction of those obtained when PGDPs are present. Furthermore, the reduced β cell tone mutes any stimuli that does not directly increase cAMP levels, including both metabolic (glucose, aa) and nonmetabolic stimuli (KCl, direct depolarization). Overall, these findings demonstrate what we believe to be a novel and expanded role for cAMP as a fundamental and essential mediator of β cell function.

The effect of PGDP to drive the appropriate amount of insulin secretion translates to whole body physiology, since mice with deletion of Gcgr and Glp1r have glucose intolerance in response to diet-induced obesity. This is a critical point in that the fundamental problem with diabetic β cells is insufficient compensation for insulin resistance (45, 46); even very insulin-resistant subjects can maintain normal glucose tolerance if insulin secretion is amplified to meet demands. In mice with β cells that cannot respond to PGDP, insulin resistance induced by obesity causes a substantial disruption of glucose homeostasis. This observation indicates that PGDPs are an essential component of the adaptation to metabolic stress and raises the possibility that abnormal α to β cell communication contributes to variation in glucose tolerance and the development of diabetes.

In summary, we provide compelling evidence that PGDPs, acting through cAMP, determine β cell tone, which directly influences the quantity of insulin secreted in response to glucose and aa. Importantly, we demonstrate that, in isolated human and murine islets, α cell ligands for the Gcgr and Glp1r are necessary for appropriate levels of cAMP in β cells. In the absence of normal α to β cell signaling, metabolic adaptation, to high-fat feeding and obesity, is impaired, thereby causing glucose intolerance. Based on these results, current models of the regulation of insulin secretion must be extended to include the essential contribution of α cells and cAMP.
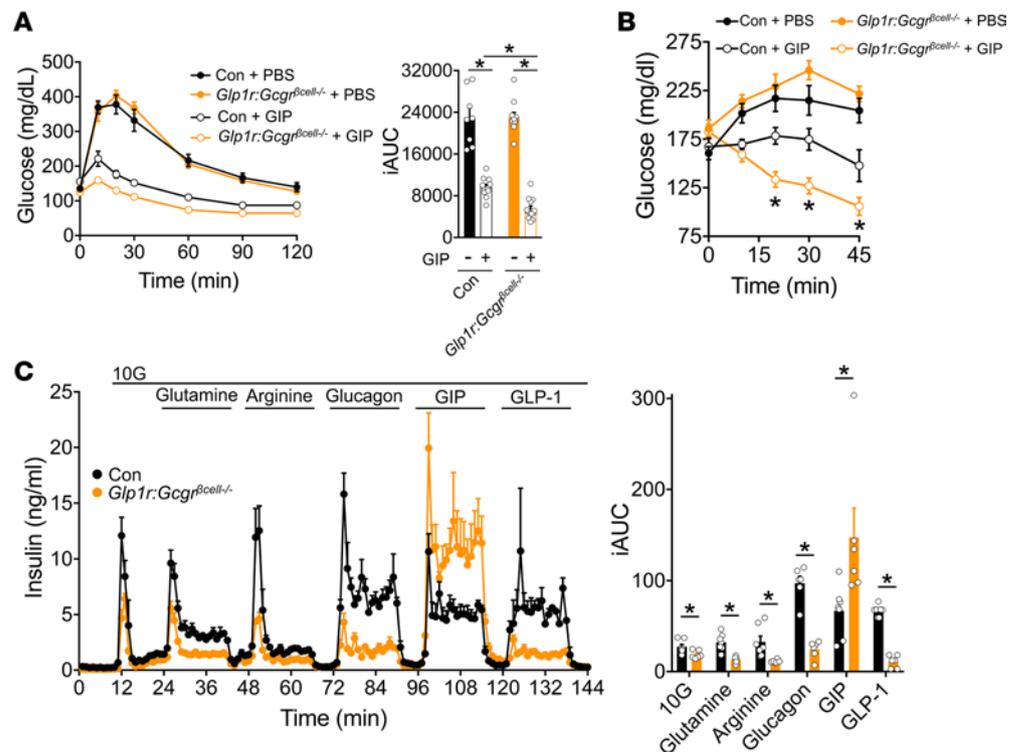
Figure 7. *Gcgr:Glp1r*^{βcell–/–} mice show an increased sensitivity to GIP in vivo and ex vivo. (**A**) i.p. glucose tolerance and iAUC from control (*n* = 11) and *Gcgr:Glp1r*^{βcell–/–} (*n* = 13) mice on a chow-diet treated with PBS or D-Ala-GIP (4 nmol/kg) 10 minutes before glucose (1.5 mg/kg). (**B**) Glycemia in ambient fed control (*n* = 9) and *Gcgr:Glp1r*^{βcell–/–} (*n* = 14) mice on chow diet after i.p. injection of PBS or D-Ala-GIP (4 nmol/kg). (**C**) Insulin secretion in response 10 mM glucose, 10 mM glutamine, 1 mM arginine, 10 nM glucagon, 3 nM GIP, and 0.3 nM GLP-1 from control (*n* = 7) or *Gcgr:Glp1r*^{βcell–/–} islets (*n* = 6). *P < 0.05. Data are shown as mean ± SEM. Data were analyzed by a 2-way ANOVA of glycemic curves (**A** and **B**) and the iAUCs (**A** and **C**).

Methods

Reagents. Glucagon and GLP-1 were purchased from MilliporeSigma, and stocks were prepared in 0.3% acetic acid. Mouse and human GIP were purchased from Chi Scientific and stocks prepared in PBS. All aa were purchased from MilliporeSigma, and fresh stocks prepared in assay buffer for each experiment. IBMX and FSK were purchased from MilliporeSigma, and stocks were prepared in DMSO. Ex9 was synthesized by GenScript, and stocks were prepared in PBS. Gcgr antibody (GRA) in PBS was provided by Kyle Sloop from Eli Lilly and Company. The Gcgr agonist 44-0410 was provided by Brian Finan from Novo Nordisk.

Animals. Experiments were performed in 8- to 24-week-old mice of the C57Bl6/J background. Mice were housed under a 12-hour light/dark cycle and provided free access to a normal chow diet. Mice harboring LoxP sites in the *Gcgr* allele (*Gcgr*^{fl}) (21, 47) were crossed with MIPcreERT (*MIP-Cre*) mice (48) to generate β cell–specific deletion of *Gcgr* (*Gcgr*^{βcell–/–}). Briefly, *MIP-Cre*^{Cre/+}:*Gcgr*^{fl/fl} mice were bred with *MIP-Cre*^{+/+}:*Gcgr*^{fl/fl} mice to produce *MIP-Cre*^{Cre/+}:*Gcgr*^{fl/fl} mice that were evenly divided to receive either oil (control) or tamoxifen (*Gcgr*^{βcell–/–}). In parallel breeding cages, *MIP-Cre*^{Cre/+} mice were bred to produce *MIP-Cre*^{+/+} and *MIP-Cre*^{Cre/+} mice that were evenly divided to receive either oil or tamoxifen. Consequently, our initial in vivo character-ization of the *Gcgr*^{βcell–/–} mice included multiple control lines (*MIP-Cre*^{Cre/+}:*Gcgr*^{fl/fl} + oil; *MIP-Cre*^{+/+}:*Gcgr*^{fl/fl} + tamoxifen, *MIP-Cre*^{+/+} + oil or tamoxifen, *MIP-Cre*^{Cre/+} + oil or tamoxifen). Tamoxifen treatment consisted of 50 mg/kg tamoxifen dissolved in corn oil administered in 6-week-old mice by oral gavage, and mice were used at least 1 month after induction. All control groups produced similar experimental results. For isolated islet experiments, control islets were from age-matched *MIP-Cre*^{Cre/+} mice treated with tamoxifen. *Glp1r*^{βcell–/–} mice were generated as described previously (22) and followed a similar breeding strategy. Control islets for *Glp1r*^{βcell–/–} mice were from age-matched *MIP-Cre*^{Cre/+} treated with tamoxifen. *Gcg*^{–/–} mice have been previously described (26). To generate experimental mice, *Gcg*^{+/-} mice were bred to produce *Gcg*^{+/+} (controls) and *Gcg*^{–/–} mice. *Gcgr;Glp1r*^{βcell–/–} mice were produced by breeding *MIP-Cre*^{+/+}:*Gcgr*^{fl/fl}:*Glp1r*^{fl/fl} and *MIP-Cre*^{Cre/+}:*Gcgr*^{fl/fl}:*Gl-*

p1r^{fl/fl} mice. Controls (*MIP-Cre^{Cre/+}*) and *Gcgr;Glp1r^{βcell–/–}* mice were given the same tamoxifen protocol described above. We choose to use *MIP-Cre^{Cre/+}* mice treated with tamoxifen as our primary control given our previous report that the *Mip-Cre* transgene produces a phenotype in the setting of high-fat diet plus streptozotocin (49). However, we have also recently reported that *MIP-Cre^{Cre/+}* mice have similar β cell function and glucose tolerance compared with *MIP-Cre^{+/+}* mice in conditions without streptozotocin when treated with either oil or tamoxifen (50), consistent with the findings present by Oropeza et al. (49). Male mice were used for all physiology experiments, and both male and female mice were used for islet experiments. A separate analysis of male versus female islets indicated there were no effects of sex on any secretion parameters.

Glucose and meal tolerance tests. Oral and i.p. glucose tolerance tests or meal tolerance tests were performed in mice after a 5-hour fast. Glucose was administered at 1.5 g/kg in PBS, liquid Ensure was administered orally at 10 ml/kg, and glucose was measured using a glucometer (Contour). D-Ala GIP was administered i.p. at 4 nmol/kg (48). For fast-refeed experiments, mice were fasted for approximately 16 hours, and blood was collected at baseline and then 30 and 60 minutes after reintroduction of chow diet into the cage. EDTA-coated capillary tubes were used to collect blood. Mice were fed a high-fat diet containing 45 kcal% fat (Research Diets) ad libitum for 8 weeks prior to i.p. and oral glucose tolerance tests.

Islet isolation. Primary islets were isolated from mice according to previously published methods (51). Briefly, the pancreas was inflated through the pancreatic duct with 0.8 mg/ml collagenase V in HBSS. The pancreas was then excised and digested for 12 minutes at 37°C. Digestion was quenched with cold RPMI (2 mM L-glutamine, 11.1 mM glucose, 0.25% BSA, 100 U/ml penicillin, and 100 μg/ml streptomycin). Islets were separated using a Histopaque gradient. Islets recovered overnight in RPMI containing 10% FBS prior to all experiments.

Islet perifusion. After incubation, equal numbers of islets (75–100 islets) were handpicked and placed into chambers containing 2.7 mM glucose KRPH buffer (140 mM NaCl, 4.7 mM KCl, 1.5 mM CaCl$_2$, 1 mM NaH$_2$PO$_4$, 1 mM MgSO$_4$, 2 mM NaHCO$_3$, 5 mM HEPES, and 1% FA-free BSA; pH = 7.4) with 100 μl Bio-Gel P-4 Media (Bio-Rad). Islets were equilibrated for 48 minutes and then perifused in intervals based on the experimental conditions. All treatments were prepared in KRPH buffer. Insulin and glucagon content and secretion was assessed by AlphaLISA (Perkin Elmer) and assayed using the EnVision plate reader (Perkin Elmer). Total GLP-1 content and secretion was measured by ELISA (Meso Scale) and measured with a SECTOR 2400 imager (Meso Scale).

Viral reactivation of proglucagon products. Recombinant Ad-CMV-Cre (ID HM101) and Ad-CMV-βgal (ID HD701) were generated using a new modular cloning platform, pMVP, that is described elsewhere (52). In brief, cDNA for Cre and β-gal were PCR amplified to incorporate attB4r/attB3r sites and subsequently recombined into pDONR221 P4r-P3r (Invitrogen) using BP Clonase II per the manufacturer's protocol (Invitrogen) to form MultiSite Gateway Pro entry plasmids. These were then recombined with MultiSite Gateway Pro entry plasmids containing the CMV promoter and IRES2-eGFP followed by the SV40 polyadenylation signal into the adenovirus backbone pAd/PL-DEST (Invitrogen) via an overnight reaction mediated by LR Clonase II plus (Invitrogen). The reaction was then transformed into NEB 10-β competent cells (New England Biolabs), and clones containing the final adenovirus vector were isolated and validated by diagnostic restriction digests. Recombinant adenoviral plasmids were subsequently linearized with PacI, propagated in HEK293 cells, and purified using CsCl$_2$ gradients. Purified adenovirus particles were titered by A$_{260}$ and determined to be E1A deficient using a qRT-PCR screen. Immediately after islets were isolated, they were placed in RPMI containing 1 μl/ml virus for 24 hours. Islets were then allowed to recover for 48–72 hours in RPMI before being perifused.

Western blot analysis. Approximately 200–250 islets were incubated at 37°C in 2.7 mM glucose KRPH buffer for 6 hours. Islets were then treated with either vehicle or 100 μM IBMX dissolved in 2.7 mM glucose KRPH buffer for 5 minutes. Islets were washed, lysed, and frozen overnight at –20°C. On the following day, lysates were run in BCA assay (Thermo Fisher). Membranes were blocked in 5% nonfat TBST (Tween 20) milk and incubated with either Phospho-PKA substrate (Cell Signaling, 9624) or Hsp90 (Cell Signaling, 4877) antibody overnight at 4°C. Images were analyzed using Image Lab software (Bio-Rad).

Cloning and adenoviral delivery of cAMP biosensors into islet β cells. The cDNA for cAMP biosensor (Epac-S^{H189}, K$_d$ = 4 μM) was cloned (53) by Gibson Assembly (New England Biolabs) into a modified pENTR-DS shuttle vector (Invitrogen) containing the rat insulin promoter (RIP) and rabbit β-globin intron as in a previous study (54). Clonase II/Gateway (Invitrogen) was then used to prepare the full-length adenoviral construct in pAd/PL-DEST (Invitrogen), yielding β cell–specific cAMP biosensors (pAd-RIP1-Epac-S^{H189}-pA). Islets were infected immediately after isolation with 1.5 μl high-titer adenovirus for 2 hours at 37°C and then moved to fresh media overnight.

Cytosolic Ca^{2+} and cAMP imaging. Islets from wild-type or *Gcg^null* mice were imaged simultaneously; one group was prelabeled with 1 μg/ml DiR (Molecular Probes) for 10 minutes. DiR labeling had no effect on islet metabolic or Ca^{2+} oscillations (data not shown). For measurements of cytosolic Ca^{2+}, islets were either preincubated in 2.5 μM FuraRed (2.5 μM, 45 minutes; Molecular Probes, F3020) or Calbryte590 (2.5 μM, 60 minutes; AAT Bioquest, 20700) in islet media at 37°C before they were placed in a glass-bottomed imaging chamber (Warner Instruments) mounted on a Nikon Ti-Eclipse inverted microscope equipped with a ×10/0.50 NA SuperFluor objective (Nikon Instruments). The chamber was perfused with a standard external solution containing 135 mM NaCl, 4.8 mM KCl, 2.5 mM $CaCl_2$, 1.2 mM $MgCl_2$, 20 mM HEPES (pH 7.35). The flow rate was maintained at 0.25 ml/minutes using feedback control (Fluigent MCFS-EZ), and temperature was maintained at 33°C using solution and chamber heaters (Warner Instruments). Excitation was provided by a SOLA SEII 365 (Lumencor) set to 10% output. Single DiR images utilized a Chroma Cy7 cube (ET710/75x, T760lpxr, 810/90m). For FuraRed, excitation (ET430/20x and ET500/20x, ET type, Chroma Technology Corporation) and emission (650/60m) filters (BrightLine type, Semrock) were used in combination with an FF444/521/608-Di01 dichroic beamsplitter (Semrock) and reported as an excitation ratio (R430/500). The same dichroic was used for Calbryte 590, but an ET572/32x filter was used for excitation and an ET632/60m filter was used for emission. The same dichroic mirror was used for cAMP biosensor FRET imaging, with CFP excitation provided by an ET430/24x filter and emission filters for CFP and Venus emission (ET470/24m and ET535/30m, Chroma) reported as an emission ratio (R470/535). Fluorescence emission was collected with a Hamamatsu ORCA-Flash4.0 V2 Digital CMOS camera every 6 seconds. A single region of interest was used to quantify the average response of each islet using Nikon Elements.

Capacitance measurements. Islets were dispersed in calcium-free dissociation buffer and incubated overnight in 11 mM glucose RPMI. Patch clamping was performed using the standard whole-cell technique with the sine + DC lock-in function of an EPC10 amplifier and Patchmaster software (HEKA Electronics). Experiments were performed at 32°C–35°C using an extracellular bath solution (118 mM NaCl, 20 mM TEA, 5.6 mM KCl, 1.2 mM $MgCl_2$, 2.6 mM $CaCl_2$, 5 mM glucose, 5 mM HEPES, pH = 7.4 and pipette solution 125 mM CsGlutamate, 10 mM CsCl, 10 mM NaCl, 1 mM $MgCl_2$, 0.05 mM EGTA, 5 mM HEPES, 3 mM MgATP, pH = 7.15**)**), which contained either 0.1 mM cAMP or no cAMP. Capacitance responses to a train of ten 500-ms depolarizations (–70 to 0 mV) were normalized to initial cell size and expressed as femtofarad per picofarad (fF/pF). Mouse β cells were identified by size and the inactivation of a voltage-gated Na^+ current at around -90 mV.

Data availability. The data that support the findings of this study are available from the corresponding author upon reasonable request.

Statistics. All data are presented as mean ± SEM. Statistical analyses were performed using GraphPad Prism 7. A 2-tailed Student's *t* test or 1-or 2-way ANOVA was performed, depending on the experimental design, with a Bonferroni post-hoc analysis. $P < 0.05$ was determined to identify statistically significant differences.

Study approval. All mouse procedures were approved and performed in accordance with the Duke University Institutional Animal Care and Use Committee.

Author contributions

MEC, DAD, and JEC designed and directed the study. PEM and MJM contributed to the study design and the preparation of the manuscript. RWC made conceptual contributions. MEC, BS, SEE, SLL, MDD, JLJ, and HL performed experiments. JMH developed and provided viral constructs. MEC, DAD, and JEC wrote the manuscript. All authors reviewed the manuscript and provided final approval for submission.

Acknowledgments

Address correspondence to: Jonathan E. Campbell, 300 N Duke Street, Durham, North Carolina 27701, USA. Phone: 919.684.4865; Email: jonathan.campbell@duke.edu.

1. Prentki M, Nolan CJ. Islet beta cell failure in type 2 diabetes. *J Clin Invest*. 2006;116(7):1802–1812.
2. Gromada J, Franklin I, Wollheim CB. Alpha-cells of the endocrine pancreas: 35 years of research but the enigma remains. *Endocr Rev*. 2007;28(1):84–116.
3. Henquin JC, Dufrane D, Nenquin M. Nutrient control of insulin secretion in isolated normal human islets. *Diabetes*. 2006;55(12):3470–3477.
4. Campbell JE, Drucker DJ. Pharmacology, physiology, and mechanisms of incretin hormone action. *Cell Metab*. 2013;17(6):819–837.
5. Kawamori D, et al. Insulin signaling in alpha cells modulates glucagon secretion in vivo. *Cell Metab*. 2009;9(4):350–361.
6. van der Meulen T, et al. Urocortin3 mediates somatostatin-dependent negative feedback control of insulin secretion. *Nat Med*. 2015;21(7):769–776.
7. Rorsman P, Huising MO. The somatostatin-secreting pancreatic δ-cell in health and disease. *Nat Rev Endocrinol*. 2018;14(7):404–414.
8. Schuit FC, Pipeleers DG. Regulation of adenosine 3',5'-monophosphate levels in the pancreatic B cell. *Endocrinology*. 1985;117(3):834–840.
9. Wojtusciszyn A, Armanet M, Morel P, Berney T, Bosco D. Insulin secretion from human beta cells is heterogeneous and dependent on cell-to-cell contacts. *Diabetologia*. 2008;51(10):1843–1852.
10. Huypens P, Ling Z, Pipeleers D, Schuit F. Glucagon receptors on human islet cells contribute to glucose competence of insulin release. *Diabetologia*. 2000;43(8):1012–1019.
11. Rodriguez-Diaz R, et al. Alpha cells secrete acetylcholine as a non-neuronal paracrine signal priming beta cell function in humans. *Nat Med*. 2011;17(7):888–892.
12. Rodriguez-Diaz R, et al. Paracrine interactions within the pancreatic islet determine the glycemic set point. *Cell Metab*. 2018;27(3):549–558.e4.
13. Svendsen B, et al. Insulin secretion depends on intra-islet glucagon signaling. *Cell Rep*. 2018;25(5):1127–1134.e2.
14. Brubaker PL, Drucker DJ. Structure-function of the glucagon receptor family of G protein-coupled receptors: the glucagon, GIP, GLP-1, and GLP-2 receptors. *Recept Channels*. 2002;8(3-4):179–188.
15. Moens K, Flamez D, Van Schravendijk C, Ling Z, Pipeleers D, Schuit F. Dual glucagon recognition by pancreatic beta-cells via glucagon and glucagon-like peptide 1 receptors. *Diabetes*. 1998;47(1):66–72.
16. Curry DL. Glucagon potentiation of insulin secretion by the perfused rat pancreas. *Diabetes*. 1970;19(6):420–428.
17. Turner DS, McIntyre N. Stimulation by glucagon of insulin release from rabbit pancreas in vitro. *Lancet*. 1966;1(7433):351–352.
18. Kilimnik G, Kim A, Steiner DF, Friedman TC, Hara M. Intraislet production of GLP-1 by activation of prohormone convertase 1/3 in pancreatic α-cells in mouse models of ß-cell regeneration. *Islets*. 2010;2(3):149–155.
19. Marchetti P, et al. A local glucagon-like peptide 1 (GLP-1) system in human pancreatic islets. *Diabetologia*. 2012;55(12):3262–3272.
20. Unger RH. Glucagon physiology and pathophysiology. *N Engl J Med*. 1971;285(8):443–449.
21. Rivero-Gutierrez B, et al. Deletion of the glucagon receptor gene before and after experimental diabetes reveals differential protection from hyperglycemia. *Mol Metab*. 2018;17:28–38.
22. Smith EP, et al. The role of β cell glucagon-like peptide-1 signaling in glucose regulation and response to diabetes drugs. *Cell Metab*. 2014;19(6):1050–1057.
23. Gerich JE, Charles MA, Grodsky GM. Characterization of the effects of arginine and glucose on glucagon and insulin release from the perfused rat pancreas. *J Clin Invest*. 1974;54(4):833–841.
24. Dean ED, et al. Interrupted glucagon signaling reveals hepatic α cell axis and role for L-glutamine in α cell proliferation. *Cell Metab*. 2017;25(6):1362–1373.e5.
25. Kim J, et al. Amino acid transporter Slc38a5 controls glucagon receptor inhibition-induced pancreatic α cell hyperplasia in mice. *Cell Metab*. 2017;25(6):1348–1361.e8.
26. Chambers AP, et al. The role of pancreatic preproglucagon in glucose homeostasis in mice. *Cell Metab*. 2017;25(4):927–934.e3.
27. Henquin JC. Triggering and amplifying pathways of regulation of insulin secretion by glucose. *Diabetes*. 2000;49(11):1751–1760.
28. Schwede F, et al. Rp-cAMPS prodrugs reveal the camp dependence of first-phase glucose-stimulated insulin secretion. *Mol Endocrinol*. 2015;29(7):988–1005.
29. Flamez D, et al. Altered cAMP and Ca2+ signaling in mouse pancreatic islets with glucagon-like peptide-1 receptor null phenotype. *Diabetes*. 1999;48(10):1979–1986.
30. Tian G, Sol ER, Xu Y, Shuai H, Tengholm A. Impaired cAMP generation contributes to defective glucose-stimulated insulin secretion after long-term exposure to palmitate. *Diabetes*. 2015;64(3):904–915.
31. Bosco D, et al. Unique arrangement of alpha- and beta-cells in human islets of Langerhans. *Diabetes*. 2010;59(5):1202–1210.
32. Kahn SE, et al. Quantification of the relationship between insulin sensitivity and beta-cell function in human subjects. Evidence for a hyperbolic function. *Diabetes*. 1993;42(11):1663–1672.
33. Pederson RA, et al. Enhanced glucose-dependent insulinotropic polypeptide secretion and insulinotropic action in glucagon-like peptide 1 receptor -/- mice. *Diabetes*. 1998;47(7):1046–1052.
34. Nauck MA, Heimesaat MM, Orskov C, Holst JJ, Ebert R, Creutzfeldt W. Preserved incretin activity of glucagon-like peptide

1 [7-36 amide] but not of synthetic human gastric inhibitory polypeptide in patients with type-2 diabetes mellitus. *J Clin Invest*. 1993;91(1):301–307.

35. Xu G, et al. Downregulation of GLP-1 and GIP receptor expression by hyperglycemia: possible contribution to impaired incretin effects in diabetes. *Diabetes*. 2007;56(6):1551–1558.

36. Nauck M, Stöckmann F, Ebert R, Creutzfeldt W. Reduced incretin effect in type 2 (non-insulin-dependent) diabetes. *Diabetologia*. 1986;29(1):46–52.

37. Nauck MA, et al. Incretin effects of increasing glucose loads in man calculated from venous insulin and C-peptide responses. *J Clin Endocrinol Metab*. 1986;63(2):492–498.

38. Campbell JE, Drucker DJ. Islet α cells and glucagon--critical regulators of energy homeostasis. *Nat Rev Endocrinol*. 2015;11(6):329–338.

39. Traub S, et al. Pancreatic α cell-derived glucagon-related peptides are required for β cell adaptation and glucose homeostasis. *Cell Rep*. 2017;18(13):3192–3203.

40. Pipeleers DG, in't Veld PA, Van de Winkel M, Maes E, Schuit FC, Gepts W. A new in vitro model for the study of pancreatic A and B cells. *Endocrinology*. 1985;117(3):806–816.

41. Pipeleers DG, et al. Interplay of nutrients and hormones in the regulation of insulin release. *Endocrinology*. 1985;117(3):824–833.

42. Pipeleers DG, Schuit FC, Van Schravendijk CF, Van de Winkel M. Interplay of nutrients and hormones in the regulation of glucagon release. *Endocrinology*. 1985;117(3):817–823.

43. Tengholm A. Cyclic AMP dynamics in the pancreatic β-cell. *Ups J Med Sci*. 2012;117(4):355–369.

44. Ferdaoussi M, et al. Isocitrate-to-SENP1 signaling amplifies insulin secretion and rescues dysfunctional β cells. *J Clin Invest*. 2015;125(10):3847–3860.

45. Bell GI, Polonsky KS. Diabetes mellitus and genetically programmed defects in beta-cell function. *Nature*. 2001;414(6865):788–791.

46. Kahn SE, Cooper ME, Del Prato S. Pathophysiology and treatment of type 2 diabetes: perspectives on the past, present, and future. *Lancet*. 2014;383(9922):1068–1083.

47. Kim T, et al. Hepatic glucagon receptor signaling enhances insulin-stimulated glucose disposal in rodents. *Diabetes*. 2018;67(11):2157–2166.

48. Campbell JE, et al. TCF1 links GIPR signaling to the control of beta cell function and survival. *Nat Med*. 2016;22(1):84–90.

49. Oropeza D, et al. Phenotypic characterization of MIP-CreERT1Lphi mice with transgene-driven islet expression of human growth hormone. *Diabetes*. 2015;64(11):3798–3807.

50. Douros JD, et al. Enhanced glucose control following vertical sleeve gastrectomy does not require a β-cell glucagon-like peptide 1 receptor. *Diabetes*. 2018;67(8):1504–1511.

51. Lamont BJ, Li Y, Kwan E, Brown TJ, Gaisano H, Drucker DJ. Pancreatic GLP-1 receptor activation is sufficient for incretin control of glucose metabolism in mice. *J Clin Invest*. 2012;122(1):388–402.

52. Haldeman JM, et al. Creation of versatile cloning platforms for transgene expression dCas9-based epigenome editing [published online ahead of print December 27, 2018]. Nucleic Acids Res. https://doi.org/10.1093/nar/gky1286.

53. Klarenbeek J, Goedhart J, van Batenburg A, Groenewald D, Jalink K. Fourth-generation epac-based FRET sensors for cAMP feature exceptional brightness, photostability and dynamic range: characterization of dedicated sensors for FLIM, for ratiometry and with high affinity. *PLoS One*. 2015;10(4):e0122513.

54. Merrins MJ, Van Dyke AR, Mapp AK, Rizzo MA, Satin LS. Direct measurements of oscillatory glycolysis in pancreatic islet β-cells using novel fluorescence resonance energy transfer (FRET) biosensors for pyruvate kinase M2 activity. *J Biol Chem*. 2013;288(46):33312–33322.